Tight Gas Reservoir Dynamic Reserve Calculation with Modified Flowing Material Balance Method

Jie He
Northwest University
Xiangdong Guo
Yanchang Oilfield Oil and Gas Exploration Company
Hongjun Cui
Yanchang Oilfield Oil and Gas Exploration Company
Kaiyu Lei
Yanchang Oilfield Oil and Gas Exploration Company
Yanyun Lei
Yanchang Oilfield Oil and Gas Exploration Company
Lin Zhou
Northwest University
Qinghai Liu
Northwest University
Yushuang Zhu (petroleum_gas@163.com)
Northwest University
Linyu Liu
Northwest University

Research Article

Keywords: Dynamic reserve, Flowing material Balance, Tight gas reservoir, Yan'an Gas field, Ordos Basin

Posted Date: June 23rd, 2021

DOI: https://doi.org/10.21203/rs.3.rs-616580/v1

Tight gas reservoir dynamic reserve calculation with modified flowing material balance method

Jie He[1], Xiangdong Guo[2], Hongjun Cui[2], Kaiyu Lei[2], Yanyun Lei[2], Lin Zhou[1], Qinghai Liu[1], Yushuang Zhu[1], Linyu Liu[1]

1. State Key Laboratory of Continental Dynamics/Department of Geology, Northwest University, Xi'an, 710069, China;

2. No. 1 Gas Production Plant, Yanchang Oilfield Oil and Gas Exploration Company, Yan'an 716000, China;

Corresponding author: Yushuang Zhu, Professor, Doctoral Supervisor, Northwest University, China. **E-mail address:** petroleum_gas@163.com.

Abstract: The determination of dynamic reserves of gas well is an important basis for rational production allocation and development of a single well. The commonly used flow material balance method (FMB method) uses the slope of the curve of wellhead pressure and cumulative production after stable production of gas well to replace the slope of the curve of average formation pressure and cumulative production to calculate the controlled reserves of single well. However, based on the theoretical calculation, the FMB method ignores the change of natural gas compression coefficient, viscosity and deviation coefficient in the production process. After considering these changes, the slope of the curve of the relationship between bottom hole pressure and cumulative production and the slope of the curve of the relationship between average formation pressure and cumulative production are not equal. In order to solve this problem, the influence of pressure on each parameter is considered, and the equation of modified flowing material balance method is derived. The application of Yan'an gas field in Ordos Basin shows that: compared with the results of the material balance method, the result of the flow material balance method is smaller, and the maximum error is 58.816%. The consequence of the modified mobile material balance method is more accurate, and the average error is 2.114%, which has good applicability. This study provides technical support for an accurate evaluation of dynamic reserves of tight gas wells in Yan'an gas field, and has important guiding significance for economic and efficient development of gas reservoir.

Keywords: Dynamic reserve; Flowing material Balance; Tight gas reservoir; Yan'an Gas field; Ordos Basin

0 Introduction

Yan'an gas field, located in the southeast of Yishan slope in Ordos Basin, is a typical tight sandstone gas reservoir with the characteristics of low permeability, strong heterogeneity, strong stress sensitivity and complex percolation mechanism(Li and Qiao, 2012). Pressure measurement and variable production often occur in the process of production test and development, so it is difficult to calculate the dynamic reserves of gas wells in this gas field.

At present, the main methods for calculating dynamic reserves including material balance method, the production decline method, production accumulation method, elastic two-phase method and so on(Chen and Che, 2011; Shults, 2020). Among them, the establishment of the material balance method is relatively easy, and only needs high-pressure property data and production data, the calculation method is relatively simple(Cheng et al., 2005; Yang et al., 2019). Therefore, this method has become a commonly used one for dynamic analysis of gas reservoirs and is widely used in various gas reservoirs at home and abroad.

When there is no data such as bottom hole pressure, the material balance method cannot calculate the dynamic reserves of gas wells. In order to solve this problem, Mattar put forward the flowing material balance method, which is analyzed from the point of view of percolation mechanics (Yang et al., 2019; Yin et al., 2019). For a closed gas reservoir, after the gas well is produced relatively stable for a certain period of time, the pressure wave is transmitted to the outer boundary of the formation, and gas seepage enters a pseudo steady state(Huang et al., 2015). As showed in the figure (Fig. 1), the pressure drop curve will be some parallel curves, and the formation pressure drop is almost equal to the bottom hole flow pressure drop in the same period of time(He et al., 2019). When gas wells are produced with stable production, there is a stable conversion relationship between bottom hole flow pressure and wellhead casing pressure, Mattar et al proposed that wellhead casing pressure and bottom hole flow pressure replace formation pressure in generalized material balance respectively:

$$\frac{P_c}{Z} = \frac{P_{ci}}{Z_i}\left(1 - \frac{G_p}{G}\right) \qquad \text{Formula (1)}$$

$$\frac{P_{wf}}{Z}=\frac{P_{wfi}}{Z_i}\left(1-\frac{G_p}{G}\right) \qquad \text{Formula (2)}$$

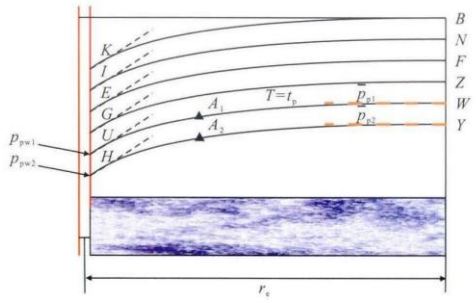

Fig. 1 Diagram of pseudo-steady-state production of gas well

The flowing material balance method does not take into account the effect of pressure on the viscosity and compression coefficient of gas, that is, it is considered that the viscosity and compression coefficient of natural gas remain unchanged(Yu et al., 2012). However, when the formation pressure of the reservoir is low and the production pressure difference is large, the assumption is not valid, so there is an error in the calculation(Han et al., 2019; Zhang et al., 2013b; Zhong et al., 2012).

In order to solve the above problems, a modified FMB method is proposed in this study, in which the influence of pressure on the viscosity and compression coefficient of gas is considered, and the modified flowing material balance equation is derived. Taking the tight gas reservoir in Yanchang Oilfield in Ordos Basin as an example, the flow material balance method before and after correction is compared and analyzed, and the accuracy of the modified flow material balance method is verified.

1 Method

1.1 Property of natural gas

1.1.1 Viscosity of natural gas

The viscosity of natural gas is different from that of liquid. Under the condition of low pressure, the viscosity of natural gas increases with the increase of temperature(Yao et al., 2015). However, when the pressure is greater than 10MPa, the viscosity of natural gas decreases at first and then increases with the increase of temperature. However, whether under low pressure or high pressure, the viscosity of natural gas increases with the increase of pressure. When there is non-hydrocarbon gas in natural gas, the viscosity often increases.

The experimental determination of natural gas is difficult, so reservoir engineers usually use relevant empirical formulas to calculate(Wei et al., 2017). Through 10 natural gas samples (Table. 1) under the condition of temperature 352 K and pressure 30MPa, the viscosity is calculated, and the pressure-viscosity diagram is drawn based on the calculated results, as showed in figure (Fig. 2).

1.1.2 Deviation coefficient of natural gas

The deviation coefficient of natural gas refers to the ratio of the real volume to the ideal volume of the same mass gas under a certain temperature and pressure(Wei et al., 2017). Through the data of 10 gas samples, we can get the relationship between Z at different temperatures, as showed in figure (Fig. 3). When the pressure is lower than 15MPa, Z decreases with the increase of pressure, and then increases with the increase of temperature.

$$Z = V_{\text{actual}} / V_{\text{ideal}}$$

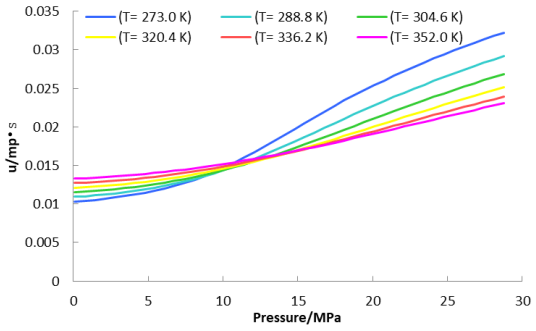

Fig. 2 P-μ curve of natural gas

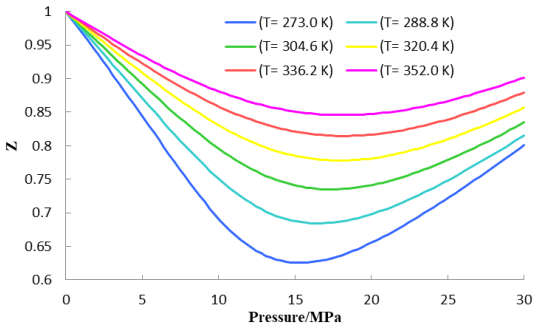

Fig. 3 P-Z curve of natural gas

1.1.3 Compression coefficient of natural gas

The compression coefficient of natural gas refers to the change of unit volume with pressure under the condition of constant temperature(Nie et al., 2018). For ideal gas, Z=1, therefore, Cg=1/P(Zhang et al., 2013a).

$$C_g = -\frac{1}{V}\left(\frac{\partial V}{\partial p}\right)_T$$

According to the data of 10 samples, the relationship of P~Cg at different temperatures can be obtained, as showed in figure (Fig. 4): the compression coefficient of gas decreases with temperature and pressure, and is less affected by temperature.

1.1.4 Volume coefficient of natural gas

The volume of natural gas is measured under the surface standard conditions, so it is necessary to convert the volume of natural gas measured under the surface conditions to the volume under the formation conditions(LIU, 2009; Nie et al., 2018). This conversion coefficient is the volume coefficient of natural gas. The volume coefficient of natural gas is defined as the actual volume occupied by a certain molar amount of gas under formation conditions, divided by the volume occupied by the same molar amount of gas underground standard conditions, the calculation formula is as follows:

$$B_g = \frac{V_R}{V_{sc}}$$

According to the data of 10 samples, the relationship of P~Bg at different temperatures can be obtained, as shown in figure (Fig. 5): the volume coefficient of natural gas decreases with the increase of pressure and increases with the increase of temperature.

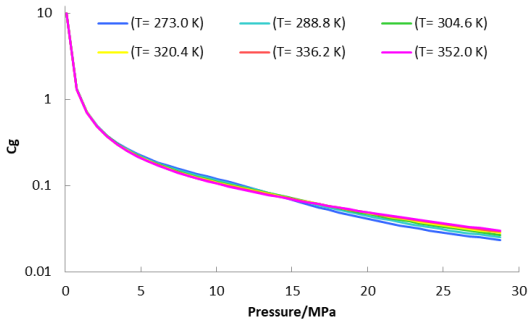

Fig. 4 P-Cg curve of natural gas

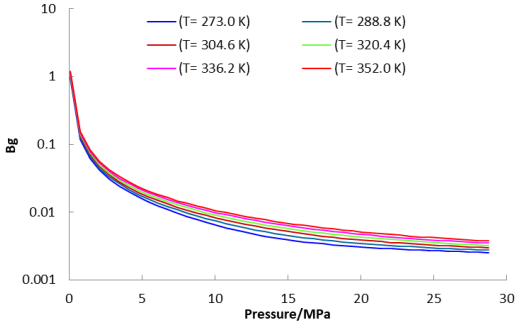

Fig. 5 P-Bg curve of natural gas

Table. 1 Composition analysis data of 10 groups of natural gas samples

Gas composition	Sample									
	1	2	3	4	5	6	7	8	9	10
C1	95.04	95.96	95.18	94.45	95.41	95.72	95.62	95.31	96.00	96.06
C2	0.47	0.59	0.44	0.53	0.45	0.49	0.68	0.55	0.50	0.55
C3	0.03	0.07	0.03	0.03	0.03	0.03	0.05	0.04	0.04	0.04
n-C4	0.03	0.07	0.05	0.04	0.05	0.03	0.16	0.13	0.12	0.13
i-C4	0	0.007	0	0	0	0	0	0	0	0
n-C5	0	0	0	0	0	0	0	0	0	0
i-C5	0	0	0	0	0	0	0	0	0	0
C6	0	0	0	0	0	0	0	0	0	0
$C7^+$	0	0	0	0	0	0	0	0	0	0
CO_2	3.84	2.68	3.66	4.33	3.06	2.83	3.04	3.34	2.83	2.63
He	0	0	0	0	0	0	0	0	0	0
H_2	0	0	0	0	0	0	0	0	0	0

H_2S	0	0	0	0	0	0	0	0	0	0
N_2	0.589	0.621	0.641	0.624	1.01	0.902	0.56	0.725	0.596	0.679
O_2	0	0	0	0	0	0	0	0	0	0
Relative density(T=20℃)	0.60	0.59	0.60	0.60	0.59	0.59	0.59	0.59	0.59	0.59
Density (T=20℃)(kg/m^3)	0.72	0.71	0.72	0.73	0.71	0.71	0.71	0.72	0.71	0.71
Low calorific value (T=20℃)(MJ/kg)	44.63	46.01	44.81	44.03	45.23	45.60	45.61	45.12	45.84	46.02
High calorific value (T=20℃)(MJ/kg)	49.54	51.06	49.73	48.87	50.20	50.61	50.62	50.09	50.88	51.08
Total	100.00	100.00	100.00	100.00	100.00	100.00	100.11	100.09	100.08	100.09

1.2 FMB method

For the gas reservoir produced by circular, closed and central vertical well, when the development stage enters the pseudo steady state, it can be obtained(Xin et al., 2018):

$$\frac{\partial\left(\overline{P}/\overline{u_g}\,\overline{C_g}\,\overline{Z}\right)}{\partial G_P}=\frac{\partial\left(\overline{P_{wf}}/u_{gwf}c_{gwf}\overline{Z}_{wf}\right)}{\partial G_P} \qquad \text{Formula (3)}$$

In the FMB method, it is assumed that the pressure has no effect on the viscosity and compression coefficient of natural gas, that is:

$$\partial\left(\overline{u_g}\,\overline{c_g}\right)=\partial\left(u_{gwf}c_{gwf}\right) \qquad \text{Formula (4)}$$

And then get:

$$\frac{\partial\left(\overline{P}/\overline{Z}\right)}{\partial G_P}=\frac{\partial\left(\overline{P}_{wf}/\overline{Z}_{wf}\right)}{\partial G_P} \qquad \text{Formula (5)}$$

Therefore, when the gas reservoir reaches pseudo steady state, $\overline{P}/\overline{Z}:G_p$ is parallel to $P_{wf}/Z_{wf}:G_p$ in Cartesian coordinate system. According to the P_{wf}/Z_{wf} and G_p data in production, the data points showing a straight line trend are fitted, and then a parallel line is made through the P_i/Z_i point, and the intercept of the parallel line on the G_p coordinate is the dynamic reserve G_i.

1.3 Modified FMB method

According to the experimental data, the composition and experimental conditions of gas are shown in the table (Table. 1) as shown. The experimental results are shown in figures (Fig. 2, Fig. 3, Fig. 4, Fig. 5). It can be seen that the viscosity, compression coefficient and deviation factor of natural gas change obviously with pressure.

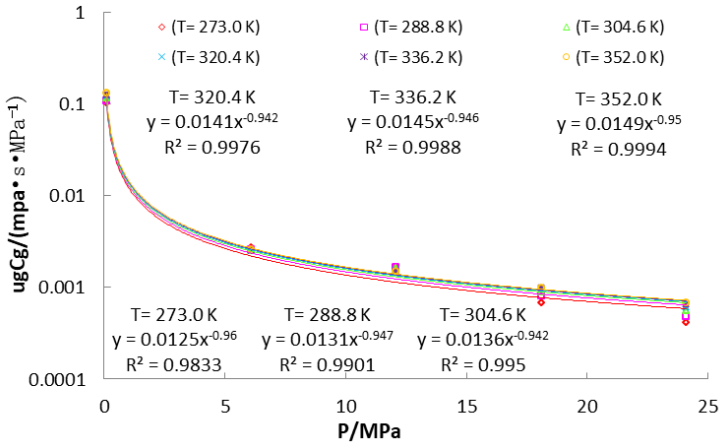

Fig. 6 P - $u_g c_g$ curve of natural gas in Yan'an gas field

The relationship between μgCg and pressure can be obtained from the experimental data. As shown in figure (Fig. 6), it can be seen that the hypothetical formula (4) is not valid, that is, the viscosity and compression coefficient of natural gas vary with pressure.

As can be seen from the figure (Fig. 6):

$$\left|\partial\left(\overline{u_g}\,\overline{c_g}\right)\right| < \left|\partial\left(u_{gwf} c_{gwf}\right)\right| \qquad \text{Formula (6)}$$

Combined with the formula (3), (6), and then get:

$$\frac{\partial\left(\overline{P}/\overline{Z}\right)}{\partial G_P} < \frac{\partial\left(P_{wf}/Z_{wf}\right)}{\partial G_P} \qquad \text{Formula (7)}$$

It can be seen that the absolute value of the slope of the P_{wf}/Z_{wf} : G_p line is greater than that of the $\overline{P}/\overline{Z}$: G_p line, and the lower the formation pressure is, the greater the production pressure difference is, and the greater the difference between them is. Therefore, reserves determined by the FMB method are smaller than the real reserves. In order to reduce the calculation error of gas well reserves, the FMB method must be modified.

By deforming the formula (3), and then get:

$$\frac{\partial\left(\overline{P}/\overline{Z}\right)}{\partial G_P} = \frac{\partial\left(\overline{u_g}\,\overline{C_g}\right)}{\partial\left(u_{gwf} c_{gwf}\right)} \mathrm{g} \frac{\partial\left(P_{wf}/Z_{wf}\right)}{\partial G_P} \qquad \text{Formula (8)}$$

It is assumed that in any short period at the initial stage of pseudo steady state, $\overline{P_{pss}}$

and p_{wf-pss} represent the average formation pressure and bottom hole flow pressure at the initial stage of pseudo steady state, respectively, $\lambda = \partial\left(\overline{u_g}\,\overline{c_g}\right) \Big/ \partial\left(u_{gwf} c_{gwf}\right)$. In the pseudo steady state, the average formation pressure and bottom hole flow pressure decrease at the same speed, so it can be considered that λ remains basically unchanged. At the same time, λ can be calculated by the P_{wf-pss} values of $u_g c_g$ and $\overline{P_{pss}}$ at the initial stage of pseudo steady state. In addition, after the gas well starts production, it will soon reach a pseudo steady state, so there is little difference between the original formation pressure and the average initial formation pressure $\overline{P_{pss}}$ of the pseudo steady state. In the pseudo steady state, λ can be calculated from the following formula:

$$\frac{\partial\left(\overline{u_g}\,\overline{C_g}\right)}{\partial\left(u_{gwf} c_{gwf}\right)} \approx \frac{\left(u_g C_g\right)\Big|_{\overline{P_{pss}}}}{\left(u_g C_g\right)\Big|_{P_{wf}-pss}} \approx \frac{\left(u_g C_g\right)\Big|_{p_i}}{\left(u_g C_g\right)\Big|_{P_{wf}-pss}} = \lambda \qquad \text{Formula (9)}$$

And then get:

$$\frac{\partial\left(\overline{P}/\overline{Z}\right)}{\partial G_P} = \lambda \frac{\partial\left(P_{wf}/Z_{wf}\right)}{\partial G_P}$$

Based on the above process, application steps of the modified FMB method are as follows (Fig. 7).

(1) according to the p : $u_g c_g$ relation curve. $\left(u_g c_g\right)\Big|_{pi}$ and $\left(u_g c_g\right)\Big|_{p_{wf-pss}}$ are determined, the formula (3-13) is determined, and the R is calculated.

(2) using the bottom hole flow pressure and cumulative production data, draw the P_{wf}/Z_{wf} : G_p curve, linearly fit the data points showing a linear trend, and determine the fitting straight line slope $-m$.

(3) calculate the $-\lambda m$, and take this slope as the slope and make a straight line over P_i/Z_i, and the intercept of the straight line on the Abscissa is the reserves determined by the modified FMB method (modified G_i).

(4) similarly, the wellhead casing pressure P_c is used to replace the bottom hole flow

pressure P_{wf}.

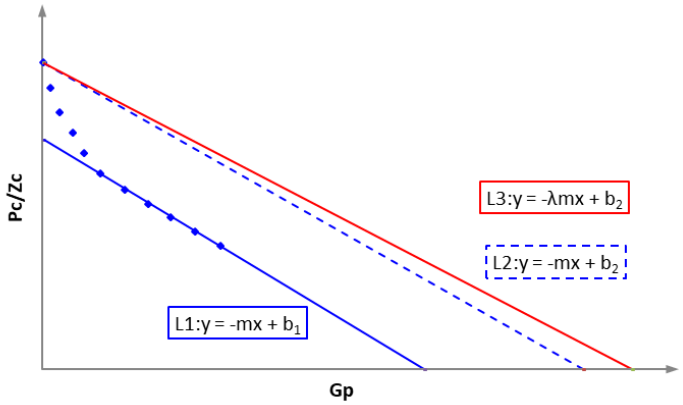

Fig. 7 Schematic diagram of dynamic reserves determined by modified FMB method

3 Result

3.1 Geological background

Ordos basin is a large sedimentary basin with multi-cycle evolution and multi-sedimentary types(Hu and Zhai, 2010). The area of the basin is about $25\times10^4 km^2$. At present, the structure is a large syncline with slow width in the east and steep and narrow in the west, and the dip angle is generally less than 1°(Li et al., 2012; Li et al., 2013). Fault folds in the margin of the basin are well developed and the internal structure is relatively simple(Liu, 2012). There is no secondary structure in the basin, and the tertiary structure is dominated by nose uplift, and there are few anticline structures with large amplitude and good trap(LIU, 2009). According to the current structural shape, basement properties and structural characteristics of the basin, the Ordos basin can be divided into six first-order structural units: Yimeng uplift, Weibei uplift, western Shanxi flexure fold belt, Yishan slope, Tianhuan depression and western margin thrust structural belt(Peng and Zhao, 2013).

Yan'an gas field is located in the southeast of Yishan slope in Ordos basin, as shown in figure (Fig. 8)(Yang et al., 2012). The comprehensive geological study shows that the Upper Paleozoic in the study area has many favorable conditions, such as extensive hydrocarbon generation, development of reservoir rock multi-layer system, wide distribution of regional caprock and so on, which are beneficial to the formation and enrichment of large lithologic gas reservoirs(Wang et al., 2011; Wang et al.,

2013).

A total of 689 gas wells in the study area are divided into three types according to the results of gas test data, and their productivity is evaluated respectively: type I wells (open flow rate > $10.0\times10^4m^3/d$), type II wells (open flow rate $4.0\sim10.0\times10^4m^3/d$) and class III wells (open flow rate less than $4.0\times10^4m^3/d$). The classification results are shown in the table (Table. 2)(Lu et al., 2019; Sun et al., 2021; Wang et al., 2017):

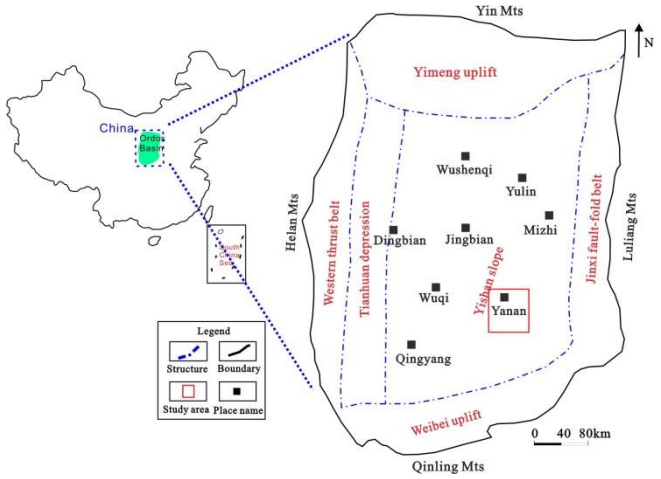

Fig. 8 Location map of Yan'an gas field in Ordos Basin

Table. 2 Classification results of gas wells in the study area

Well area	>10×10⁴m³			4～10×10⁴m³			<4×10⁴m³		
	Average (10^8m^3)	Well	Proportion (%)	Average (10^8m^3)	Well	Proportion (%)	Average (10^8m^3)	Well	Proportion (%)
Average	27.94	194	31.36	6.10	134	20.05	1.52	361	48.59

3.2 Calculation results of type I wells

The initial production of type I wells in Yan'an gas field is high, the pressure drops slowly, and the stable production time is long, so it has a good stable production capacity under the condition of low pressure.

S-4 well is a typical type I well in Yan 128 high pressure well area, and the open flow rate of gas test is $26.57\times10^4m^3/d$. It has been in production since August 2013. From the production curve (Fig. 9), it can be seen that at the initial stage of production (August 2013 to April 2015), the average monthly production of gas wells is $64\times10^4m^3/m$, and the water production is at a low level, with an average monthly production of $4.28m^3/m$, and the water-gas ratio is maintained at 0.066 ($m^3/10^4m^3$).In the second stage of production (May 2015 to April 2017), the casing pressure

decreases rapidly, the oil pressure decreases rapidly, the monthly water production is higher, and the monthly gas production decreases rapidly. In the third stage of production (May 2017 to April 2020), the monthly gas production and monthly water production are kept at a low level, casing pressure is about 7MPa, and the oil pressure is about 8MPa. Up to now, the cumulative gas production of S-4 well is $3633.775\times10^4m^3$ and the cumulative water production is $356.67m^3$.

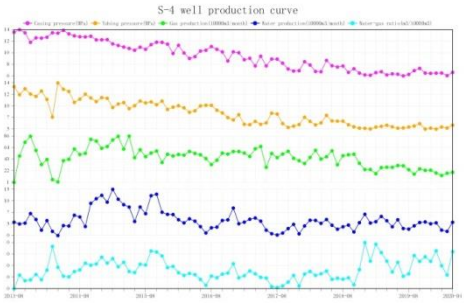

Fig. 9 S-4 well production curve

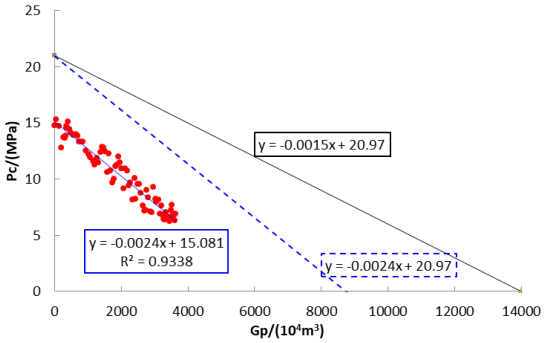

Fig. 10 S-4 calculation results of dynamic reserves

Using production data and wellhead casing pressure, draw Pc/Zc~Gp curve, as shown in figure (Fig. 10). The linear fitting is carried out for the data points showing a straight line trend, and the slope of the straight line is -0.0024. The slope of the straight line passes through the Pi/Zi point as a straight line, and the intercept on the Abscissa is $0.8737\times10^8m^8$, which is the dynamic reserve of S-4 well determined by the FMB method.

The calculation results show that $-\lambda=-0.6387$, $-\lambda m=-0.0015$. Taking $-\lambda m$ as the slope and making a straight line through the Pi/Zi point, the intercept on the Abscissa is $1.3980\times10^8m^8$, which is the dynamic reserve of well S-4 determined by the modified FMB method.

3.3 Calculation results of type II wells

The test production of type II wells in the study area is between $4.0\times10^4m^3/d$ and $10.0\times10^4m^3/d$, and the pressure drops rapidly, accounting for 20.048% of the number of wells in the whole area.

S-5 well is a typical type II well in Yan 128 high pressure well area (Fig. 11). 190 days of trial production operation was carried out in S-5 well from November 19, 2009 to May 27, 2010, and 70 days of pressure recovery test was carried out from May 27 to

August 7, 2010. The open flow rate of gas test in this well is $4.7045\times10^4m^3/d$, and the original formation pressure is 25.872 MPa. The production starts at $1.5\times10^4m^3/d$. Due to the large pressure fluctuation in the trial production process, the gas production is difficult to be stable, and the working system is adjusted, the daily gas production is gradually reduced to about $1\times10^4m^3/d$, and the daily water production is 0.1～1.8 m^3/d. After the gas production is reduced to $1\times10^4m^3/d$, the oil pressure decreases from 14.41MPa to 12.36MPa, a decrease of 2.05 MPa, and the oil pressure decreases at a rate of 0.051MPa/d, which shows that the production is basically stable. Up to April 2020, the cumulative gas production is $3471.62\times10^4m^3$ and the cumulative water production is $490.25m^3$.

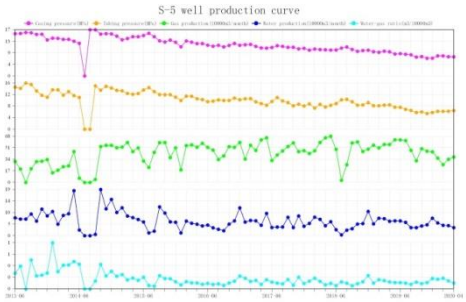

Fig. 11 S-5 well production curve

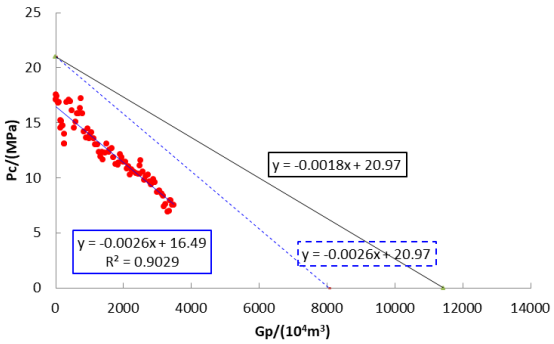

Fig. 12 S-5 calculation results of dynamic reserves

Using production data and wellhead casing pressure, draw Pc/Zc~Gp curve, as shown in figure (Fig. 12). The linear fitting is carried out for the data points showing a straight line trend, and the slope of the straight line is -0.0026. The slope of the straight line passes through the Pi/Zi point as a straight line, and the intercept on the Abscissa is $0.8065\times10^8m^8$, which is the dynamic reserve of S-5 well determined by the FMB method.

The calculation results show that -λ=-0.704, -λm=-0.0018. Taking -λm as the slope and making a straight line through the Pi/Zi point, the intercept on the Abscissa is $1.1650\times10^8m^8$, which is the dynamic reserve of well S-5 determined by the modified FMB method.

3.4 Calculation results of type III wells

The initial production of type III wells in the study area is low, about $35\times10^4m^3/m$, and the current production is $20\times10^4m^3/m$. It has a certain stable production capacity

under the condition of low pressure. If the allocation of production is reduced, it can be produced steadily for a long time.

S-6 well is a typical type III well in this area, and the open flow rate of gas test is $8.944\times10^4m^3/d$. It has been in production since June 2013. From the production curve (Fig. 13), it can be seen that at the initial stage of production (June 2013 to December 2014), the average monthly production of gas wells is $50\times10^4m^3/m$, the water production is at a low level, the average monthly production is $3.02m^3/m$, and the water-gas ratio is maintained at 0.060 ($m^3/10^4m^3$). In the second stage of production (from January 2015 to June 2018), the casing pressure decreased rapidly and the monthly gas production remained unchanged. In the third stage of production (July 2018 to April 2020), the monthly gas production decreases rapidly, the monthly water production increases rapidly, the casing pressure is kept at about 8.5MPa, and the oil pressure is maintained at about 7.8MPa. Up to now, the cumulative gas production of S-6 is $2580.92\times10^4m^3$, and the cumulative water production is $237.55m^3$.

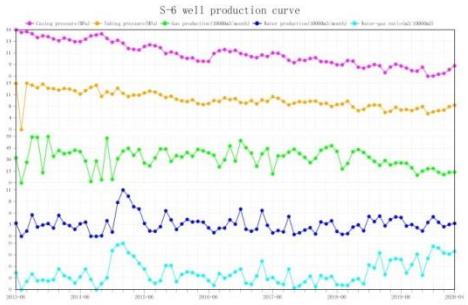

Fig. 13 S-6 well production curve

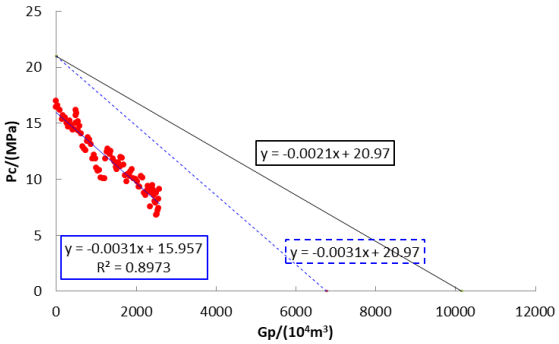

Fig. 14 S-6 calculation results of dynamic reserves

Using production data and wellhead casing pressure, draw Pc/Zc~Gp curve, as shown in figure (Fig. 14). The linear fitting is carried out for the data points showing a straight line trend, and the slope of the straight line is -0.0031. The slope of the straight line passes through the Pi/Zi point as a straight line, and the intercept on the Abscissa is $0.6765\times10^8m^8$, which is the dynamic reserve of S-6 well determined by the FMB method.

The calculation results show that $-\lambda=-0.667$, $-\lambda m=-0.0021$. Taking $-\lambda m$ as the slope and making a straight line through the Pi/Zi point, the intercept on the Abscissa is $0.9986\times10^8m^8$, which is the dynamic reserve of well S-6 determined by the modified

296 FMB method.

297 **4 Discussion**

298 Compared with the FMB method, the material balance method uses the average
299 formation pressure data measured after shut-in for a long time, so its calculation result
300 is more real and reliable(Fan et al., 2012; GAO et al., 2009).

301 **4.1 Method verification**

302 In order to verify the accuracy of the calculation results of the modified FMB method,
303 as shown in the table (Table. 3), using the measured formation pressure at different
304 stages of the production of the three wells, the scatter diagram between the cumulative
305 gas production and the measured Pzag Z is drawn (Fig. 15, Fig. 16, Fig. 17).

306 By linear fitting these discrete data points, the dynamic reserves of single well
307 calculated by three kinds of well material balance method can be obtained(Xu et al.,
308 2014; Xu et al., 2016). ① The dynamic reserve of single well in S-4 is
309 $1.3849\times10^{8}m^{8}$ calculated by material balance method. By comparing the above
310 calculation results, the error of FMB method is 36.91%, and the error of modified
311 FMB method is 0.95% (Table. 4, Fig. 18).②The dynamic reserve of single well in S-5
312 is $1.1864\times10^{8}m^{8}$ calculated by material balance method. By comparing the above
313 calculation results, the error of FMB method is 32.02%, and the error of modified
314 FMB method is 1.80 % (Table. 4, Fig. 18).③The dynamic reserve of single well in S-6
315 is $1.0086\times10^{8}m^{8}$ calculated by material balance method. By comparing the above
316 calculation results, the error of FMB method is 32.93%, and the error of modified
317 FMB method is 1.00 % (Table. 4, Fig. 18).

318 Through the above calculation results (Fig. 18), compared with the material balance
319 method, the calculation result of the FMB method is generally small, with an average
320 error of 33.95%; the error of the modified FMB method is small, with an average of
321 1.25%(Li et al., 2018). Therefore, it can be concluded that when there is a lack of
322 measured pressure data, the calculation result of the modified FMB method is more
323 accurate than that of the FMB method.

324 Table. 3 Measured pressure in three wells

Time	S4	S5	S6

	Gp(10^4m^3)	P(MPa)	P/Z	Gp(10^4m^3)	P(MPa)	P/Z	Gp(10^4m^3)	P(MPa)	P/Z
201312	268.355	18.800	20.567	135.008	18.923	20.727	216.712	18.713	20.515
201406	434.815	18.276	20.018	265.966	18.386	20.091	450.907	18.281	20.023
201412	787.525	17.918	19.589	431.721	18.147	19.893	546.945	17.644	19.321
201506	1211.685	17.617	19.152	720.386	17.578	19.273	767.195	17.980	19.659
201512	1522.465	16.668	18.186	990.256	17.360	18.988	971.055	16.738	18.231
201606	1836.965	16.488	17.915	1278.196	16.565	18.069	1200.765	16.678	18.048

325

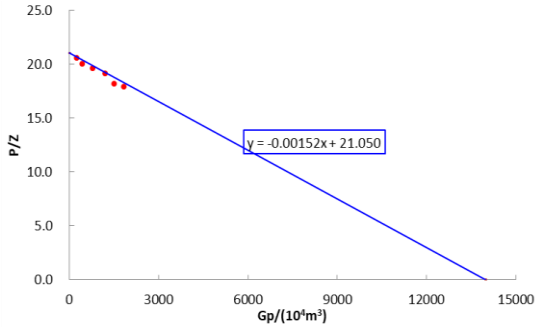

Fig. 15 calculation of dynamic reserves by pressure drop method

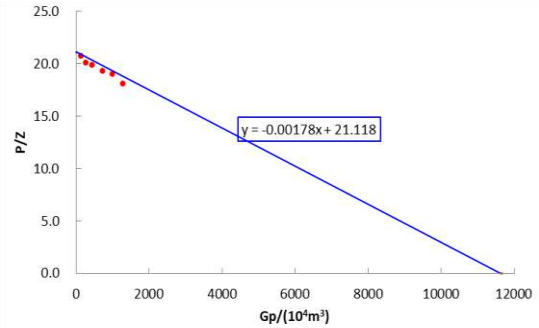

Fig. 16 calculation of dynamic reserves by pressure drop method

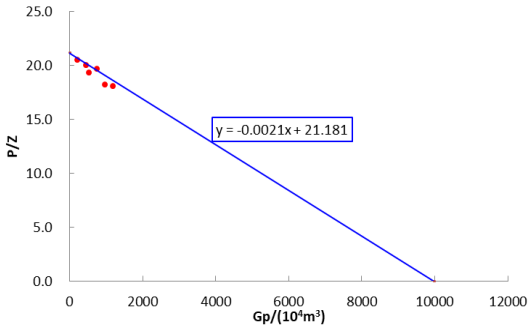

Fig. 17 calculation of dynamic reserves by pressure drop method

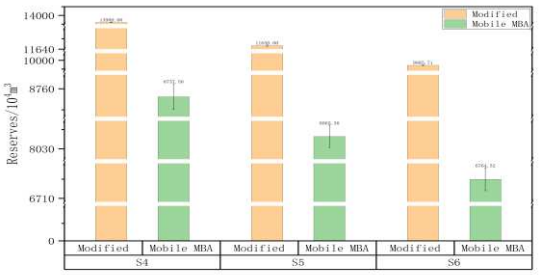

Fig. 18 Calculation error of dynamic reserves

326 Table. 4 Calculation results of FMB method and modified FMB method

Well	MBA(10^4m^3)	Mobile MBA(10^4m^3)	Error(%)	Modified Mobile MBA(10^4m^3)	Error(%)
S4	13848.68	8737.50	36.91	13980.00	0.95
S5	11864.04	8065.38	32.02	11650.00	1.80
S6	10086.19	6764.52	32.93	9985.71	1.00
Average	11932.97	7855.80	33.95	11871.90	1.25

327 **4.2 Application**

328 Three dynamic reserve methods are used to calculate 31 typical gas wells in the study
329 area, and the results are shown in the table (Table. 5). The average reserves calculated
330 by the material balance method and the FMB method are $1.2731\times10^8m^8$ and
331 $0.6794\times10^8m^8$, respectively. The minimum error is 28.499%, the maximum is
332 58.816%, and the average is 44.536%. The average error of the modified FMB

method is $1.3008\times10^{8}m^{8}$, the minimum error is 1.290%, the maximum value is 3.063%, and the average is 2.114%. It is worth noting that the single wells with large errors in the calculation results of the modified FMB method are S-56 and S-60-1.

Combined with the production data of two wells, S-56 well was put into production in June 2013 (Fig. 19), and the shut-in state appeared intermittently from June 2013 to December 2016, the pressure recovery state was in a short time, which reflected that the formation pressure and casing pressure drop in the early stage of production were relatively small, and the gas production per unit pressure drop was relatively large(Mattar et al., 2006). Because there is no intermittent shut-in in the later stage of production, the law of monthly gas production verifies this theory. Therefore, it can be concluded that the early shut-in leads to the large dynamic reserves of a single well. Similarly, the S-60-1 well was put into production in July 2015 (Fig. 20), and the intermittent shut-in occurred in the later stage of production, and the production law of the gas well could not fully reflect the real state of the gas well, resulting in a large calculation error.

It can be seen that the great change in the production system of gas wells will affect the accuracy of the calculation results of the modified FMB method, especially the shut-in for a long time before calculating the pressure drop gas production at a certain time. Therefore, time data points with relatively stable production should be selected as far as possible to calculate the dynamic reserves of a single well.

Table. 5 Calculation results of three dynamic reserve methods

WELL	Initial wellhead casing pressure(MPa)	Pseudo steady wellhead casing pressure(MPa)	MBA	Mobile MBA		Modified Mobile MBA	
			Reserves (10^4m^3)	Reserves (10^4m^3)	Error(%)	Reserves (10^4m^3)	Error(%)
S1	15.8462	12.8592	7153.74	4282.75	40.133%	7342.40	2.637%
S12	17.1079	13.4597	14160.04	6336.27	55.252%	14370.62	1.487%
S14	18.7003	12.8507	10602.13	5843.84	44.881%	10833.20	2.179%
S15	17.3198	14.2056	12111.63	8659.90	28.499%	12334.85	1.843%
S16	18.0042	14.2344	12881.02	6668.23	48.232%	13183.31	2.347%
S18	20.9695	14.9531	9300.99	5114.52	45.011%	9482.64	1.953%
S19	19.1588	13.4765	15158.98	7982.84	47.339%	15426.74	1.766%
S2	16.6048	12.7247	4488.28	2515.88	43.946%	4560.57	1.611%
S20	20.9194	15.9530	23281.23	11621.87	50.081%	23693.58	1.771%

S23	17.2632	12.3611	18463.87	11508.79	37.669%	18979.53	2.793%
S24	17.8761	13.3496	8295.53	4831.38	41.759%	8488.67	2.328%
S3	15.3464	11.4357	4419.17	3009.09	31.908%	4498.07	1.785%
S36	16.7579	13.4424	14231.18	9857.57	30.733%	14547.33	2.222%
S37	20.8429	15.2572	8776.13	4631.75	47.223%	8951.42	1.997%
S38	15.3464	12.7981	17870.36	10961.70	38.660%	18146.58	1.546%
S39	16.4099	11.9387	7545.85	3907.11	48.222%	7699.04	2.030%
S40	20.4163	15.6005	8117.51	3343.29	58.814%	8310.90	2.382%
S41	17.7460	12.0839	9631.05	5070.29	47.355%	9871.88	2.500%
S42	20.1747	15.6066	12423.66	5933.73	52.239%	12605.25	1.462%
S47	15.4740	11.0778	9600.02	5951.53	38.005%	9782.98	1.906%
S48	19.7822	14.7414	8301.62	5187.84	37.508%	8495.94	2.341%
S53	18.1943	13.6024	10815.71	6273.89	41.993%	11010.45	1.801%
S53-1	16.5886	14.4144	3168.25	1987.80	37.259%	3213.64	1.433%
S56	17.5138	14.1972	7124.17	4230.08	40.623%	7339.25	3.019%
S60	22.6343	17.3155	12818.85	5956.40	53.534%	12984.22	1.290%
S60-1	23.8290	15.3464	14704.97	7073.23	51.899%	15155.41	3.063%
S8	17.9103	13.5156	62126.78	25586.07	58.816%	63747.11	2.608%
Y170	17.9788	14.2530	16910.98	11236.74	33.554%	17356.94	2.637%
Y185	19.8759	13.2931	2211.32	1129.31	48.930%	2257.58	2.092%
Y196	18.4994	10.9542	19406.76	9736.50	49.829%	19839.12	2.228%
Y202	18.1875	13.3156	8538.40	4208.89	50.706%	8750.41	2.483%
Min	15.3464	10.9542	2211.32	1129.31	28.499%	2257.58	1.290%
Max	23.8290	17.3155	62126.78	25586.07	58.816%	63747.11	3.063%
Average	18.3638	13.6973	12730.33	6794.81	44.536%	13008.37	2.114%

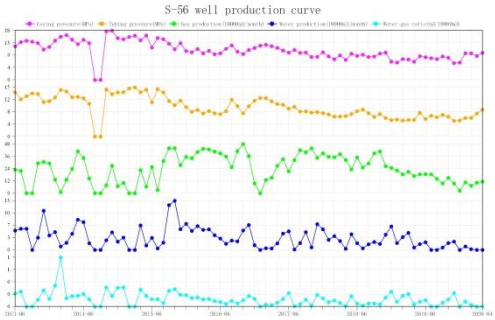

Fig. 19 S-56 well production curve

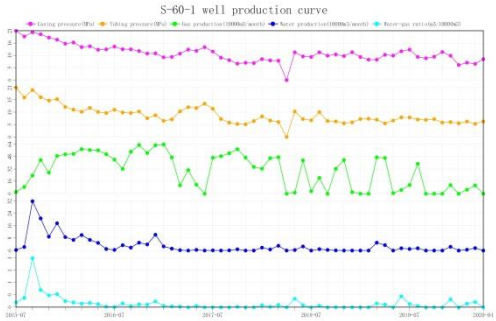

Fig. 20 S-60-1 well production curve

5 Conclusion

(1) Yan'an gas field is characterized by low permeability and strong heterogeneity. A total of 689 gas wells in the study area are divided into three types according to the results of gas test data, and their productivity is evaluated respectively: type I wells (open flow rate > $10.0\times10^4 m^3/d$), type II wells (open flow rate $4.0\sim10.0\times10^4 m^3/d$)

and class III wells (open flow rate less than $4.0\times10^4 m^3/d$).

(2) Through theoretical calculation and numerical simulation, it is found that the viscosity of natural gas increases rapidly with the increase of pressure, the compression coefficient of natural gas decreases at first (P<15MPa) and then increases with the increase of pressure (P>15MPa), and increases with the increase of temperature. Under the condition of low pressure, the compression coefficient and volume coefficient of natural gas decrease rapidly with the increase of pressure and increase with the increase of temperature.

(3) Considering the viscosity, compression coefficient and deviation coefficient of natural gas, the FMB method is modified, and the calculation method and steps are given at the same time.

(4) Verified by the production data of three types of typical gas wells, the results show that compared with the calculation results of the material balance method, the average error of the FMB method is 33.95%, and the average error of the modified FMB method is 1.25%.

(5) The new method is used to calculate the dynamic reserves of 31 gas wells in the study area. the results show that the great change of the production system of gas wells will affect the accuracy of the modified FMB method, especially the shut-in for a long time before the pressure drop gas production is calculated at a certain time, so the points with relatively stable production should be selected as far as possible to calculate the dynamic reserves of a single well.

Remarks

Z: Deviation coefficient of natural gas；

V_{actual}: The volume of a real gas, m^3;

V_{ideal}: The volume of ideal gas, m^3;

Cg: Natural gas compression coefficient；

Bg: Volume coefficient of natural gas；

V_R: Underground volume of natural gas, m^3；

Vsc: Volume of natural gas under surface conditions, m^3；

P_c: Wellhead casing pressure, MPa；

P_{ci} : Original wellhead casing pressure, MPa；

P_{wf} : Bottom hole flow pressure, MPa；

P_{wfi} : Original bottom hole flow pressure, MPa。

G_p : Cumulative gas production, 10^4m^3；

$\overline{P}$: Average formation pressure, MPa；

p_{wf} : Bottom hole flow pressure, MPa；

$\overline{Z}$: Deviation coefficient of natural gas under average formation pressure；

Z_{wf} : Deviation coefficient of natural gas under bottom hole flow pressure；

$\overline{u_g}$: Viscosity of natural gas under average formation pressure, mPa·s；

u_{gwf} : Viscosity of natural gas under bottom hole flow pressure, mPa·s；

$\overline{C_g}$: Compression coefficient of natural gas under average formation pressure, MPa^{-1}；

C_{gwf} : Compression coefficient of natural gas under bottom hole flow pressure, MPa^{-1}。

$\overline{P_{pss}}$: Average formation pressure at the initial stage of pseudo steady state, MPa；

P_{wf-pss} : Bottom hole flow pressure at the initial stage of pseudo steady state, MPa；

P_i : Original formation pressure, MPa；

u_g : Viscosity of natural gas, mPa·s；

C_g : Compression coefficient of natural gas, MPa^{-1}；

λ : $\left(\overline{u_g}\,\overline{c_g}\right)\Big/\left(u_{gwf}c_{gwf}\right)$。

Acknowledgement

This study was supported by the National Major Project (2017ZX05008-004-004-001). The authors would like to thank the editors and anonymous reviewers for their valuable suggestions for this paper.

Author contributions

Hongjun Cui, Lin Zhou and Qinghai Liu performed the experiments. Jie He, Xiangdong Guo and Kaiyu Lei wrote the main manuscript. Yushuang Zhu and Linyu Liu advised the students and corrected the manuscript. All authors reviewed the

manuscript.

Competing interests

The authors declare no competing interests.

Reference

Chen, G. and Che, X., 2011. Domain Material Balance Method for Low Permeability Gas-Oil Reservoir by Depletion Drive Process. Xinjiang Petroleum Geology, 32(2): 157-159.

Cheng, S., Li, J., Li, X., Yang, F. and Wang, Y., 2005. Estimation of Gas Well Dynamic Reserves by Integration of Material Balance Equation with Binomial Productivity Equation. Xinjiang Petroleum Geology, 26(2): 181-182.

Fan, X., Liu, B., Bao, J., Kui, M. and Cao, J., 2012. Dynamic Analysis of Influencing Factors of Reserves in the Sebei 1 Gas Field. Natural Gas Geoscience, 23(5): 939-943.

GAO, Q.-f., Dang, Y.-q., LI, J.-t., Yang, S.-b. and Shen, S.-f., 2009. Dynamic Reserves Calculation and Evaluation of Sebei Gas Field in Qaidam Basin. Xinjiang Petroleum Geology, 30(4): 499-500.

Han, G. et al., 2019. Determination of pore compressibility and geological reserves using a new form of the flowing material balance method. Journal of Petroleum Science and Engineering, 172: 1025-1033.

He, Z., Li, S., Zhang, F., Zhang, Q. and Li, B., 2019. Application of Dynamic Reserve Analysis in the Recovery of Fault-Block Water Invasion Reservoir. Special Oil & Gas Reservoirs, 26(6): 98-102.

Hu, W. and Zhai, G., 2010. Practice and sustainable development of oil and nature gas exploration and development in Ordos Basin. Engineering Science, 12(5): 64-72.

Huang, Q. et al., 2015. Study on theoretical basis of "flowing" material balance. Reservoir Evaluation and Development, 5(5): 30-33,49.

Li, S. and Qiao, D., 2012. Current situation of tight sand gas in China. In: Q.J. Xu, H.H. Ge and J.X. Zhang (Editors), Natural Resources and Sustainable Development, Pts 1-3. Advanced Materials Research, pp. 85-+.

Li, X. et al., 2018. Correlation between per-well average dynamic reserves and initial absolute open flow potential (AOFP) for large gas fields in China and its application. Petroleum Exploration and Development, 45(6): 1088-1093.

Li, Y., Zhong, J., Li, X., Xu, J. and Chen, X., 2012. Characteristics of lower Jurassic tight sandstone gas reservoirs in Baka area of Tuha Basin. Special Oil & Gas Reservoirs, 19(2): 29-32,136.

Li, Z., Jiang, Z., Pang, X., Li, F. and Zhang, B., 2013. Genetic Types of the Tight Sandstone Gas Reservoirs in the Kuqa Depression,Tarim Basin,NW China. Earth Science, 38(1): 156-164.

Liu, R., 2012. Discussion on the Dynamic Reserve Calculation in Early Development Stage of Gas Reservoir. Special Oil & Gas Reservoirs, 19(5): 69-72.

LIU, X.-h., 2009. A discussion on several key parameters of gas reservoir dynamic reserves calculation. Natural Gas Industry, 29(9): 71-74.

Lu, K. et al., 2019. Dynamic reserves calculated by linear relationship in the early development of water-drive gas reservoir. Lithologic Reservoirs, 31(1): 153-158.

Mattar, L., Anderson, D. and Stotts, G., 2006. Dynamic material balance - oil- or gas-in-place without shut-ins. Journal of Canadian Petroleum Technology, 45(11): 7-10.

Nie, X., Chen, J. and Yuan, S., 2018. Experimental Study on Stress Sensitivity Considering Time Effect for Tight Gas Reservoirs. Mechanika, 24(6): 784-789.

Peng, S. and Zhao, W., 2013. The adaptability study for developing tight gas reservoirs using horizontal wells. In: L. Zheng et al. (Editors), Applied Materials and Technologies for Modern

Manufacturing, Pts 1-4. Applied Mechanics and Materials, pp. 614-617.
Shults, O., 2020. Method for calculating material balance of complex process flowcharts. Journal of Mathematical Chemistry, 58(6): 1281-1290.
Sun, H. et al., 2021. A material balance based practical analysis method to improve the dynamic reserve evaluation reliability of ultra-deep gas reservoirs with ultra-high pressure. Natural Gas Industry B.
Wang, J. et al., 2011. Characteristic of Tight Sandstone Gas Reservoir in Tuha Basin and Its Exploration Target. Xinjiang Petroleum Geology, 32(1): 14-17.
Wang, M., Fan, Z., Luo, W., Song, H. and Ding, J., 2017. Error Analysis of Dynamic Reserve Calculation in Multi-Layer Loose Sandstone Gas Reservoir. Special Oil & Gas Reservoirs, 24(6): 100-106.
Wang, Y. et al., 2013. Comparison of Ordos and Foreign Similar Basins and Prediction for Mesozoic Oil Reserves in Ordos Basin. Geoscience, 27(5): 1244-1250.
Wei, X. et al., 2017. New geological understanding of tight sandstone gas. Lithologic Reservoirs, 29(1): 11-20.
Xin, C., Wang, Y., Xu, Y., Shi, L. and Du, Y., 2018. Tight Gas Reservoir Dynamic Reserve Calculation with Modified Flowing Material Balance. Special Oil & Gas Reservoirs, 25(2): 95-98.
Xu, M., Ran, Q., Li, N. and Shen, G., 2014. Effect of Sealed Boundary on Fluid Flow in Fractured Well in Deformable Tight Gas Reservoir. Special Oil & Gas Reservoirs, 21(5): 92-94.
Xu, Y., Adefidipe, O. and Dehghanpour, H., 2016. A flowing material balance equation for two-phase flowback analysis. Journal of Petroleum Science and Engineering, 142: 170-185.
Yang, H., Fu, J., Liu, X. and Meng, P., 2012. Accumulation conditions and exploration and development of tight gas in the Upper Paleozoic of the Ordos Basin. Petroleum Exploration and Development, 39(3): 295-303.
Yang, X., Lei, Y., Ma, D., Wang, L. and Wen, H., 2019. Application of new method of calculating dynamic reserves in Bohai Oilfield. Fault Block Oil & Gas Field, 26(3): 329-332.
Yao, J. et al., 2015. Gas Control Factors and Evaluation Application of Tight Sandstone Gas Reservoirs. Well Logging Technology, 39(4): 482-485,490.
Yin, W., Wu, Y. and Yu, J., 2019. Key Influencing Factor Analysis of the SEC Dynamic Reserve in Liaohe Oilfield. Special Oil & Gas Reservoirs, 26(2): 86-90.
Yu, X., Liu, H., Cao, J. and Pang, J., 2012. The Research on Material Balance Considering In-Seam and Intrabed Water. In: X. Zhou and Z.Z. Lei (Editors), Fluid Dynamic and Mechanical & Electrical Control Engineering. Applied Mechanics and Materials, pp. 420-+.
Zhang, L., Zhang, L., Jiang, B. and Liu, H., 2013a. The method of dynamic reserves prediction for a constant volume gas reservoir. In: G. Li and C. Chen (Editors), Applied Mechanics and Materials I, Pts 1-3. Applied Mechanics and Materials, pp. 456-+.
Zhang, L., Zhang, L., Zhang, J., Lan, F. and Deng, P., 2013b. Calculation methods of the dynamic reserves for gas wells in a low-permeability gas reservoir. In: X. Tang, W. Zhong, D. Zhuang, C. Li and Y. Liu (Editors), Progress in Environmental Protection and Processing of Resource, Pts 1-4. Applied Mechanics and Materials, pp. 3243-+.
Zhong, H., Zhou, J., Li, Y., Pu, H. and Tan, Y., 2012. Dynamic reserve calculation of single well of low permeability gas reservoir based on flowing material balance method. Lithologic Reservoirs, 24(3): 108-111.